Journal of Pharmaceutical Analysis 14 (2024) 101002

Contents lists available at ScienceDirect

Journal of Pharmaceutical Analysis

journal homepage: www.elsevier.com/locate/jpa

Original article

Investigation of oligomeric proanthocyanidins extracted from Rhodiolae Crenulatae Radix et Rhizomes using deep eutectic solvents and identified via data-dependent acquisition mass-spectroscopy

Li Jia [a, 1], Liming Wang [a, b, 1], Xiaoxiao Zhang [a], Qingrui Zhang [a], Peng Lei [a], Yanxu Chang [a], Lifeng Han [a], Xin Chai [a], Wenzhi Yang [a], Yuefei Wang [a, b], Miaomiao Jiang [a, b, *]

[a] National Key Laboratory of Chinese Medicine Modernization, Tianjin University of Traditional Chinese Medicine, Tianjin, 301617, China
[b] Haihe Laboratory of Modern Chinese Medicine, Tianjin University of Traditional Chinese Medicine, Tianjin, 301617, China

ARTICLE INFO

Article history:
Received 23 July 2023
Received in revised form
5 May 2024
Accepted 9 May 2024

Keywords:
Proanthocyanidins
Deep eutectic solvent
Rhodiolae Crenulatae Radix et Rhizomes
Pharmacodynamic material basis

ABSTRACT

In this study, 34 deep eutectic solvents (DESs) were successfully prepared for the extraction of proanthocyanidin from Rhodiolae Crenulatae Radix et Rhizomes. The extraction process was optimized using single factor exploration and Box-Behnken design-response surface analysis. The extraction rate was significantly improved when the molar ratio of choline chloride to 1,3-propanediol was 1:3.5 and the water content was 30% (*V*/*V*) in DESs. AB-8 macroporous resin and ethyl acetate were used for separation and refining, and the oligomer-rich proanthocyanidin components were eventually obtained. The ultraviolet (UV) and infrared (IR) spectra showed that the proanthocyanidins were mainly composed of catechin and epicatechin. To further clarify the chemical composition of proanthocyanidin, an ion scan list containing 156 proanthocyanidins precursors was obtained by constructing a proanthocyanidins structural library and mass defect filtering (MDF) algorithm, combined with the full mass spectrometry (MS)/dd-MS^2 scan mode that turns on the "if idle pick others" function. By using ultra-high performance liquid chromatography and high-resolution MS (UHPLC/HRMS), the analysis used both targeted and non-targeted methods to detect proanthocyanidins. Finally, 50 oligomeric proanthocyanidin (OPC) compounds were identified, including 7 monomers, 22 dimers, 20 trimers, and 1 tetramer, most of which were procyanidins of proanthocyanidins (84%), and a small amount of prodelphinidin (14%) and other types of proanthocyanidins (2%), which enabled the systematic characterization of proanthocyanidin components from Rhodiolae Crenulatae Radix et Rhizomes. Meanwhile, the comparison with the grape seeds OPCs standard (United States Pharmacopeia) revealed that the proanthocyanidins in Rhodiolae Crenulatae Radix et Rhizomes were more abundant, suggesting that the proanthocyanidins in Rhodiolae Crenulatae Radix et Rhizomes has promising applications.

1. Introduction

Rhodiola crenulata root and rhizome, scientifically known as *Rhodiola crenulata* (Hook. f. & Thomson) H. Ohba [1], are the dried parts of the plant used for their revitalizing effects on liver and kidney functions and for stimulating blood circulation [2]. Contemporary pharmacological research has revealed that this botanical material is rich in a spectrum of bioactive compounds, including phenylethanoid glycosides, polyphenols, flavonoids, terpenes, volatile oils, and coumarins. These constituents are recognized for their diverse therapeutic effects, including antioxidant, anti-aging, anti-fatigue, anti-cancer, and cardiovascular protective properties [3–8]. Although current studies on Rhodiola crenulata root and rhizome have predominantly concentrated on phenylethanoid glycosides, such as salidroside [9–11], there has been less emphasis on the role of proanthocyanidins. Despite being less explored, these proanthocyanidins also contribute to the antioxidant activities of the plant [12,13].

Proanthocyanidins, prevalent natural polyphenolic compounds in plants, are some of the most efficacious antioxidant substances known for their ability to scavenge free radicals when absorbed by

* Corresponding author. Haihe Laboratory of Modern Chinese Medicine, Tianjin University of Traditional Chinese Medicine, Tianjin, 301617, China.
E-mail address: miaomiaojiang@tjutcm.edu.cn (M. Jiang).
[1] Both authors contributed equally to this work.

https://doi.org/10.1016/j.jpha.2024.101002

the human body [14,15]. These compounds are composed of multi-electron hydroxyl structures, assembled through the polymerization of flavan-3-ols and their derivatives, interconnected by C4—C6 or C4—C8 bonds [16,17]. This results in various isomeric forms of proanthocyanidins with identical mass, complicating their structural characterization. The range from dimers to tetramers is known as oligomeric proanthocyanidins (OPCs), while larger assemblies from pentamers onward are termed polymeric proanthocyanidins (PPCs) [18]. The degree of polymerization is directly correlated with their antioxidant capacity. Notably, OPCs exhibit more robust antioxidant activities than both monomeric and polymeric forms, including benefits such as oxidative stress reduction, anti-lipid peroxidation, and anti-inflammatory effects [19—21]. The current standard for extracting proanthocyanidins involves the use of acetone [22,23], yet its flammability and volatility raise safety concerns in laboratory environments. Consequently, there is an imperative need to identify a safer, yet equally effective, solvent that exhibits high specificity and extraction efficiency for procuring proanthocyanidins from plant sources, ultimately aiming to replace hazardous organic solvents such as acetone.

Deep eutectic solvents (DESs) are often synthesized as homogenous, stable, and clear liquids through various processes such as heating, stirring, freeze-drying, or vacuum evaporation, combining hydrogen bond donors (HBDs) and hydrogen bond acceptors (HBAs). A growing body of research has employed DESs for the extraction of anthocyanins from plant materials. In comparison to traditional organic solvents, a DES formulated from choline chloride and 1,3-propylene glycol not only demonstrates an extraction efficiency comparable to that of acetone but also offers the benefits of reduced volatility and easier to obtain [24—29].

Liquid chromatography-mass spectrometry (LC-MS) offers unparalleled benefits for the comprehensive and systematic characterization of components in traditional Chinese medicine (TCM), making it a mainstay in foundational TCM research. It has been reported that ultra-high performance liquid chromatography (UHPLC)-photo-diode array (PDA)-electrospray ionization (ESI)/high-resolution MS (HRMS)^n can be effectively utilized to profile 247 proanthocyanidins across seven plants, with polymerization degrees ranging from monomers to pentamers. This underscores the capability of LC-MS for in-depth analysis of proanthocyanidins in Rhodiola Crenulata root and rhizome, offering a promising pathway to pinpointing potential active compounds [30,31].

In this study, we constructed a DES to replace organic solvents for the extraction of proanthocyanidins from Rhodiolae Crenulatae Radix et Rhizomes by combining a single-factor investigation with a Box-Behnken design. A proanthocyanidin precursor ion list based on a proanthocyanidin structural library and mass defect filtering (MDF) algorithm were constructed on the basis of UHPLC/HRMS. Furthermore, a full MS/dd-MS^2 scanning mode was used, and "if idle pick others" dynamic exclusion (DE) functions were simultaneously turned on to target and non-target the proanthocyanidin components in Rhodiolae Crenulatae Radix et Rhizomes to provide a new method and new idea for the reasonable use of proanthocyanidin in Rhodiolae Crenulatae Radix et Rhizomes.

2. Experimental

2.1. Reagents and materials

Reference compounds (Fig. S1) were purchased from Shanghai Yuanye Biotechnology Co., Ltd. (Shanghai, China). Methanol (Fisher Scientific, Fair Lawn, NJ, USA) was of high performance liquid chromatography (HPLC) grade and acetonitrile and formic acid (Fisher Scientific) were of LC-MS grade. Ultra-pure water (18.2 MΩ•cm at 25 °C) was in-house prepared using a Milli-Q Integral 5 water purification system (Millipore, Bedford, MA, USA). The Rhodiolae Crenulatae Radix et Rhizomes was purchased from Beijing Tongrentang Health Pharmaceutical (Ningxia) Co., Ltd. (Ningxia, China) and identified it as the dried root and rhizome of *Rhodiola crenulate* (Hook. f. et Thomson) H. Ohba, by Dr. Honghua Wu from Tianjin University of Traditional Chinese Medicine (Tianjin, China). Voucher specimens were deposited at Tianjin University of Traditional Chinese Medicine.

2.2. Construction of DES and screening of extraction conditions

In this section, we use choline chloride, betaine, and proline as HBAs and use polyols, organic acids, sugars, and amides as HBDs to select and add to the sample bottle. The magnetic stirring was conducted at 80 °C until a uniform transparent liquid was formed. The combination of solvents that formed a deep eutectic within 12 h was selected. We used viscometers (LVT-1ZN, Shanghai Ranhui Industrial Co., Ltd., Shanghai, China) to measure the viscosities of the DESs before and after the addition of water (50%, *V*/*V*), detected the Fourier transform infrared (FTIR) of the DESs before and after the addition of water (50%, *V*/*V*), and tested for pH after adding 50% (*V*/*V*) of water to each solvent to form a deep eutectic.

A precise mass of 1.00 g of Rhodiola crenulata root and rhizome powder should be weighed and 10 mL of extraction solvent added. The mixture should then be subjected to a water bath at 65 °C for 50 min, followed by centrifugation at 10,000 *g* for 10 min. The supernatant should be collected to obtain the Rhodiola crenulata extract. Extract solutions of the DESs and organic reagents should also be obtained from the supernatant. The proanthocyanidin content in the crude extract should be determined using the n-butanol and hydrochloric acid assay methods.

By altering a single variable at a time and maintaining a consistent composition of the DES, the impact of different molar ratios and water contents on the extraction rates of proanthocyanidins from Rhodiola crenulata root and rhizome was examined. Comparative studies were conducted to assess the efficiency of proanthocyanidin extraction from Rhodiola crenulata root and rhizome using various solid-liquid ratios, extraction durations, and temperatures. The optimal conditions for extracting proanthocyanidins with DES were determined through the application of the Box-Behnken design and response surface methodology.

2.3. Isolation and purification of proanthocyanidin crude extract

DES (2,500 mL), composed of choline chloride and 1,3-propanediol in a molar ratio of 1:3.5 and a water content of 30% (*V*/*V*), was used. According to the solid to liquid ratio of 1:30, 100 g of Rhodiolae Crenulatae Radix et Rhizomes medicinal powder was weighed, mixed in a beaker, extracted with a dark water bath at 40 °C for 50 min, and the extract was centrifuged at 6,000 *g* for 10 min. The supernatant was combined to obtain the crude proanthocyanidin extract. Separation was performed using an AB-8 macroporous resin. First, 3 bed volume (3 BV) was eluted with 10% ethanol, and then 3 BV of the 70% ethanol eluent was collected. After the ethanol was removed by low-temperature reduced-pressure rotary evaporation, 1.5× (*V*/*V*) ethyl acetate was used for extraction three times. The organic phase layer was collected and ethyl acetate was removed by low-temperature reduced-pressure rotary evaporation. After the ethanol was redissolved in ultrapure water, it was lyophilized to obtain a refined powder of Rhodiolae Crenulatae Radix et Rhizomes proanthocyanidin.

An appropriate amount of lyophilized proanthocyanidin powder was weighed, dissolved in methanol, and a solution of the proanthocyanidin sample was prepared at various concentrations and

scanned at a wavelength of 200–400 nm for the ultraviolet (UV) absorption spectrum. Simultaneously, lyophilized proanthocyanidin powder was blended with potassium bromide, thoroughly ground, and compressed into pellets. These pellets were then scanned by an infrared (IR) spectrometer to detect spectroscopic signals within the range of 400–4,000 cm^{-1}.

2.4. Sample preparation

An accurate mass of 5.00 mg of lyophilized proanthocyanidin powder from Rhodiola crenulata root and rhizome was weighed and redissolved in 1 mL of 70% methanol. The solution was vortexed for 2 min, then centrifuged at 15,000 *g* for 10 min at 4 °C. The supernatant was eluted using a solid-phase extraction (SPE)-C_{18} column (Tianjin Agela Technologies Co., Ltd., Tianjin, China), and the eluate was collected and concentrated under a stream of nitrogen until dry. The residue was redissolved in 200 μL of methanol, followed by a further centrifugation at 15,000 *g* for 10 min at 4 °C. A volume of 200 μL of the resulting supernatant was then transferred into an amber sample vial for subsequent analysis. The entire experimental process was conducted in the absence of light to prevent any photoinduced degradation.

An accurate mass of 1.00 mg of each standard was weighed and dissolved in 70% methanol. This solution was vortexed for 2 min to ensure thorough mixing, yielding a reference standard solution with a concentration of 1 mg/mL. This solution was then sequentially diluted to achieve a final concentration of 200 μg/mL. After dilution, the solution was centrifuged at 15,000 *g* for 10 min at 4 °C. The clarified supernatant was then carefully transferred into an amber injection vial in preparation for subsequent analysis.

2.5. Chromatographic and MS conditions

Using ACQUITY UPLC® HSS T_3 column (2.1 mm × 100 mm, 1.8 μm; Waters Corporation, Milford, MA, USA) as the stationary phase, the chromatographic conditions for the detection of proanthocyanidins were as follows: the column temperature was set at 35 °C with chromatographic column flow rate of 0.3 mL/min. Furthermore, 0.1% aqueous formic acid as phase (A) and pure acetonitrile as phase (B) were used with respect to time as follows: 0–1 min, 3%–11% (B); 1–10 min, 11%–13% (B); 10–13 min, 13%–14% (B); 13–18 min, 14%–16% (B); 18–23 min, 16%–20% (B); 23–25 min, 20%–22% (B); 25%–30 min, 22%–26% (B); 30–33 min, 26%–30% (B); 33–35 min, 30%–35% (B); 35–38 min, 35%–37% (B); 38–40 min, 37%–40% (B); 40–43 min, 40%–45% (B); 43–45 min, 45%–95% (B); and 45–47 min, 95% (B) of the elution gradient. The injection volume was 2 μL.

Mass spectral data were acquired via the Thermo Scientific Orbitrap Exploris 120 HRMS (Thermo Fisher Scientific Inc., Bremen, Germany), and negative electrospray ionization (ESI^-) source was used. The full MS/dd-MS^2 scanning mode was combined with the constructed proanthocyanidin precursor ion scanning list. Meanwhile, the “if idle pick others” function (“perform dependent scan on most intension if no targets are found”) is turned on, and the main parameters of the ion source are set as follows: spray voltage of 3,000 V, capillary temperature at 350 °C, auxiliary gas temperature at 350 °C, normalized collision energy (NCE) at 20, 40, and 60 V, sheath gas at 35 arb (sheath gas, N_2), auxiliary gas flow rate at 10 arb (auxillary gas, N_2), 0 arb purge gas (sweep gas, N_2), full MS full scan range of *m*/*z* 150–2,000, resolution of 120,000, and MS^2 scan resolution of 15,000. The DE time was set to 8.0 s, and the isolation was set to *m*/*z* 4.0 for sample data acquisition.

2.6. Data processing and analysis

The negative high energy collision dissociation (HCD)-MS^2 data of all fractionated samples were interpreted for the structural characterization of proanthocyanidins from Rhodiolae Crenulatae Radix et Rhizomes. Xcalibur software was used to read the data and predict the most probable molecular formula for each observed precursor ion. The parameters were set as follows: charge, −1; mass tolerance, 10 ppm; ring double-bound equivalent (RDB eq), 5–20, and element in use, $15 \leq C \leq 90$, $14 \leq H \leq 100$, and $6 \leq O \leq 60$.

3. Results and discussion

3.1. Construction of DES and determination of optimal extraction conditions

DESs were prepared by selecting choline chloride, betaine, proline, polyols, organic acids, sugars, and amides. As shown in Table S1, choline chloride can form DES with six organic acids, eight polyols, and urea; betaine can form DESs with five organic acids and two polyols; proline can form DESs with four organic acids and one polyol; and four organic acids can form seven DESs with two polyols. In total, 34 distinct DES formulations can be formed. The states of some DESs are shown in the upper part of Fig. 1A. The viscosity of the DESs, prepared with solid HBD, was significantly higher than that of the DESs prepared with liquid HBD. Additionally, the DESs (DES-C1, DES-C3, and DES-C5) with proline as the hydrogen bond receptor exhibited different degrees of transparent yellow color, whereas the other DESs were transparent and colorless. DES-A11 and DES-A13 exhibited needle-like crystals when placed at room temperature after DES formation, suggesting that the two DESs had high-temperature requirements and were relatively unstable at room temperature.

The pH values and properties of 34 DESs were recorded and presented in Table S2. FTIR detection of the DESs was performed both prior to and subsequent to the addition of water, with the results depicted in Fig. S2. The DESs exhibited a degree of similarity in their FTIR spectra both before and after water was added (Fig. S2A). The IR absorption peaks at 3,600 cm^{-1} and 3,200 cm^{-1} were found to be significantly enhanced following the addition of water, which was indicative of a substantial increase in the content of free and combined hydroxyl (−OH) groups. Upon detailed analysis (Fig. S2B), it was observed that the IR detection outcomes for 15 types of DESs, which utilized choline chloride as the HBA, maintained their similarity after the addition of water (50%, *V*/*V*). This observation suggested that the structural integrity of the DESs was not entirely compromised, and their molecular framework continued to be present. However, inconsistencies were noted in some DESs before and after the use of betaine or proline as the HBA, coupled with the addition of water (50%, *V*/*V*). This indicated that the introduction of a large volume of water might have the potential to disrupt the DESs' structure. Additionally, the FTIR spectra of DESs, which were composed of organic acids and polyols, were still observed to be similar before and after the addition of water (50%, *V*/*V*). This similarity suggested that these DESs retained a relatively stable structural configuration. Compared to conventional extraction solvents (organic reagents and water), DES usually exhibit higher viscosities. It was determined that the viscosity of the DES could be reduced, liquidity could be improved, and the extraction rate of the DES could be increased by adding a small amount of water. Therefore, the viscosities of the DESs before and after the addition of water (50%, *V*/*V*) were measured after uniform

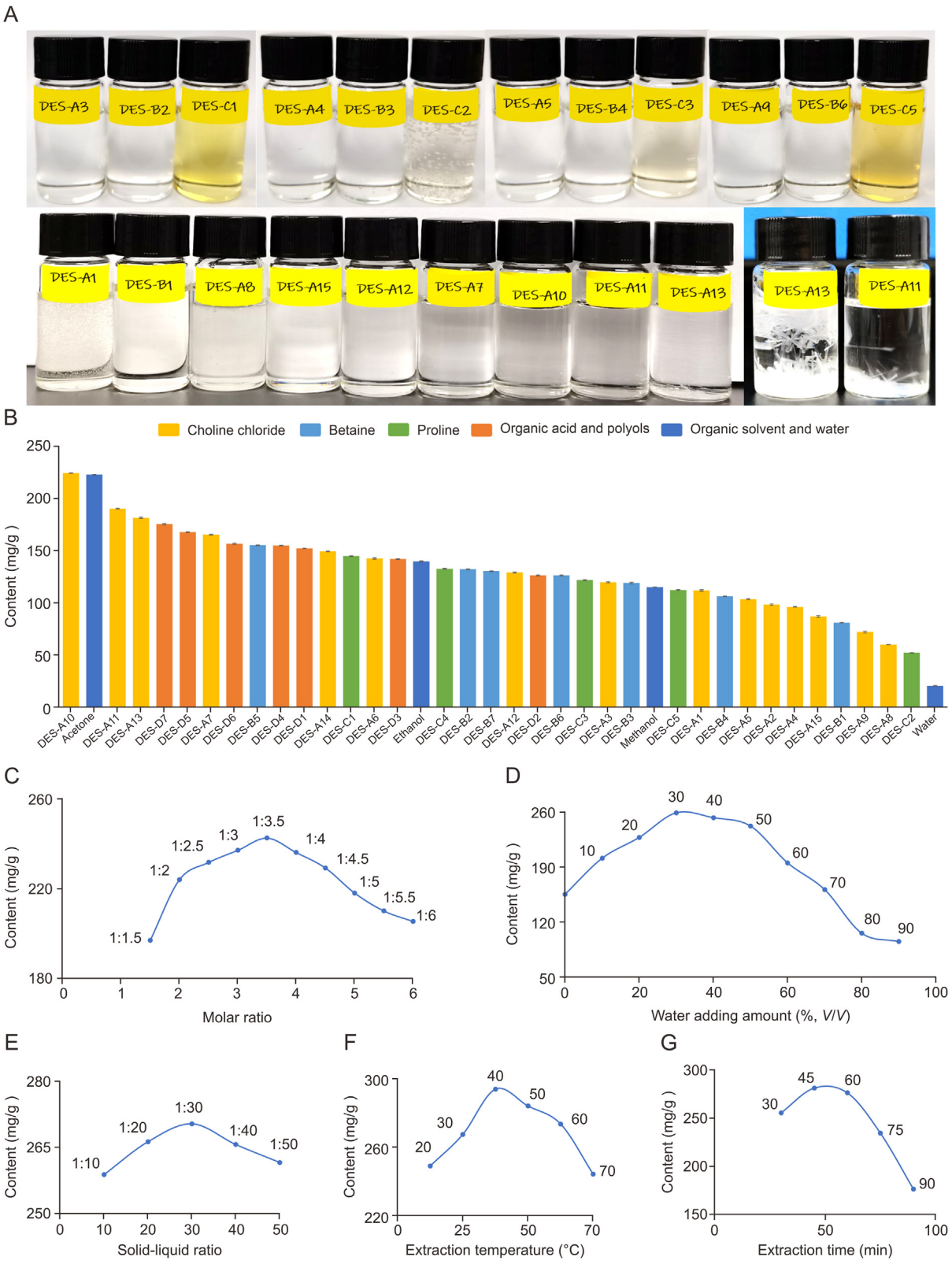

Fig. 1. Extraction of proanthocyanidin from Rhodiolae Crenulatae Radix et Rhizomes by deep eutectic solvent (DES): (A) the states of some DESs; (B) comparison of extraction amounts of proanthocyanidins from Rhodiolae Crenulatae Radix et Rhizomes extracted with 34 eutectic solvents and 4 conventional solvents; (C) different molar ratios; (D) different water addition amounts; (E) different solid-liquid ratios; (F) different extraction temperatures; and (G) different extraction times.

mixing. The results are summarized in Table S3. With the same HBD, choline chloride as HBA forms a DES more easily than betaine and proline. When organic acids (oxalic acid and malic acid) were used as HBD, the viscosity of the solvent forming the deep eutectic was relatively high, whereas most of the solvents forming the deep eutectic with polyols as HBD exhibited relatively low viscosities. The addition of ultra-pure water can obviously improve the fluidity of the DES and enhance the fluidity of the DES, which was originally poor in fluidity. DES-A11 and DES-A13, which were initially unstable at room temperature, were found to form a uniform and stable solvent upon the addition of water. This stabilization occurred because the HBA and HBD constituents were dissolved in water, thereby preventing the precipitation of needle-like crystals.

34 DESs and four conventional solvents with the same crude drug content were selected to extract proanthocyanidins from Rhodiolae Crenulatae Radix et Rhizomes. The *n*-butanol-hydrochloric acid method was used to determine the contents of the different extracts ($n = 3$). The results are summarized in Table S4. After the results are sorted, as shown in Fig. 1B, it is shown that the extraction rates of all solvents are higher than those of ultrapure water (20 mg/g). Using organic solvents for extraction, the efficiency ranked as follows: 70% acetone (222.05 mg/g) > 70% ethanol (139.31 mg/g) > 70% methanol (114.77 mg/g), which indicated that proanthocyanidins exhibit relatively low polarity. Hence, the extraction efficiency was the highest when 70% acetone were used. This result is consistent with findings in the literature [23]. Moreover, the extraction rate of HBD using polyols was higher than that using organic acids and urea as HBDs when the HBA types were the same. This can potentially be due to the fact that most polyols are liquid and have higher mobility after DES formation. Hence, they are more likely to bind to the drug and dissolve the active component. This also shows that the extraction rate of DES increases with a decrease in viscosity. Hence, when the length of the carbon chain of polyols increases [32–36], the hydrophobicity of the polyols increases and the extraction rate also decreases [37]. Among the 34 DESs, DES-A10, composed of choline chloride and 1,3-propanediol in a molar ratio of 1:2, with a water content of 50% (*V*/*V*), exhibited the highest extraction rate of 223.49 mg/g. This was almost the same as the extraction efficiency of 70% acetone (222.05 mg/g), indicating that DES-A10 had a high selectivity for proanthocyanidins in Rhodiolae Crenulatae Radix et Rhizomes. Prior to undertaking the extraction experiments, we reviewed numerous studies related to the extraction of proanthocyanidins using DES [23–39]. It was noted that Cao et al. [23] achieved an extraction rate of 22.19 ± 0.71 mg/g for proanthocyanidins from Ginkgo biloba leaves using a DES composed of choline chloride and malonic acid with a 55% (*V*/*V*) water content. However, our literature review revealed that the stability of DES can be influenced by water content. Typically, DES compositions remain relatively stable with water additions below 30%. However, as water content increases from 30% to 50% (*V*/*V*), the composition of DES can begin to change. At water levels exceeding 50% (*V*/*V*), the structure of the DES may be disrupted by the excessive water. This leads to chloride ions in the water competing for the binding sites between the DES and extracted sample, ultimately impacting the extraction rate, as highlighted in prior research [40]. The extraction efficiencies of hydrophilic and hydrophobic DES varied significantly when they were used to extract components with different properties, as highlighted in the literature [41]. To validate that the DES were responsible for the extraction, rather than a mere mixture of the HBA and HBD, we conducted control experiments. These included extractions using a 50% (*V*/*V*) aqueous solution of choline chloride (representing the HBA) and a 50% (*V*/*V*) aqueous solution of 1,3-propanediol (representing the HBD), both set to the optimal DES amounts. The comparative results with the optimal DES are depicted in Fig. S3. The data indicate that the extraction rates of proanthocyanidins from Rhodiolae Crenulatae Radix et Rhizomes using aqueous solutions of either HBA (choline chloride) or HBD (1,3-propylene glycol) were inferior to those obtained with the combined aqueous DES solution. This suggests that the addition of 50% (*V*/*V*) water diminishes the interaction between the water molecules and eutectic solvent composed of choline chloride and 1,3-propylene glycol. Moreover, compared to chloride ions, proanthocyanidins appear to interact more readily with DES species, facilitating a more effective extraction process.

The extraction performance of proanthocyanidins from Rhodiolae Crenulatae Radix et Rhizomes is evaluated using various molar ratios and water contents of DES, as depicted in Figs. 1C and D. Notably, a DES with a molar ratio of 1:3.5 (choline chloride to 1,3-propanediol) and a water content of 30% (*V*/*V*), significantly outperformed other molar ratios, yielding a higher extraction rate. This finding is detailed in Figs. 1E–G and Table S5, where these conditions are compared with other extraction scenarios. Different water addition was suggested to possibly affect the structure of DESs. Therefore, it was necessary to clarify the relationship between water addition and the DESs structure. The FTIR absorption of DES-A10 was tested under various conditions of water addition, as depicted in Fig. 2A. Upon initial observation, the FTIR spectra were found to be generally similar. However, upon closer examination, it was determined that the similarity of the FTIR spectra was higher when the proportion of water added was below 50% (*V*/*V*). Conversely, when the water content surpassed 50% (*V*/*V*), the FTIR spectra exhibited significant differences.

To further elucidate the impact of varying water addition conditions on the structure of DESs, conventional molecular dynamics (CMD) simulations were conducted on the DES-A10 under different water addition scenarios. As depicted in Fig. 2B, the molecules of choline chloride, 1,3-propanediol, and water were labeled accordingly, with the hydroxyl groups on choline designated as Hy and Oy, the terminal oxygen and hydrogen atoms of 1,3-propanediol labeled as Ot and Ht, and the hydrogen and oxygen atoms of water were identified as Hw and Ow, respectively. The interactions among water molecules, choline chloride, and 1,3-propanediol were illustrated in Fig. 2B. It was observed that when no water was added or when 10% (*V*/*V*) water addition was made, the interactions between water/choline chloride and water/1,3-propanediol were not predominant. Instead, the intermolecular hydrogen bonds between choline chloride and 1,3-propanediol remained the dominant feature, indicating that the 10% water addition was effectively integrated into the initial hydrogen bond network of the DESs without altering the hydrogen bond between choline chloride and 1,3-propanediol. Upon reaching 30% (*V*/*V*) water content, the hydrogen bonds between water/choline chloride and water/1,3-propanediol were gradually incorporated into the existing hydrogen bond network. This demonstrated that 30% (*V*/*V*) water content did not disrupt the DESs' hydrogen bond network but rather expanded it. When the water addition reached 50% (*V*/*V*), a portion of the hydrogen bond network between choline chloride and 1,3-propanediol was disrupted. This led to a shift in the hydrogen bond interaction of the DESs from inter-group to intra-group, with some interactions between choline chloride and 1,3-propanediol being suppressed, and a notable increase in the hydrogen bonds between water/choline chloride and water/1,3-propanediol. As the water addition continued to increase (70%–90%, *V*/*V*), it became evident that an excessive amount of water completely dismantled the original hydrogen bond network of the DESs. This resulted in the complete release of choline chloride and 1,3-propanediol from their original hydrogen bond network, with the formation of new hydrogen bonds between the DESs and water. The hydrogen bond interactions occur between choline chloride

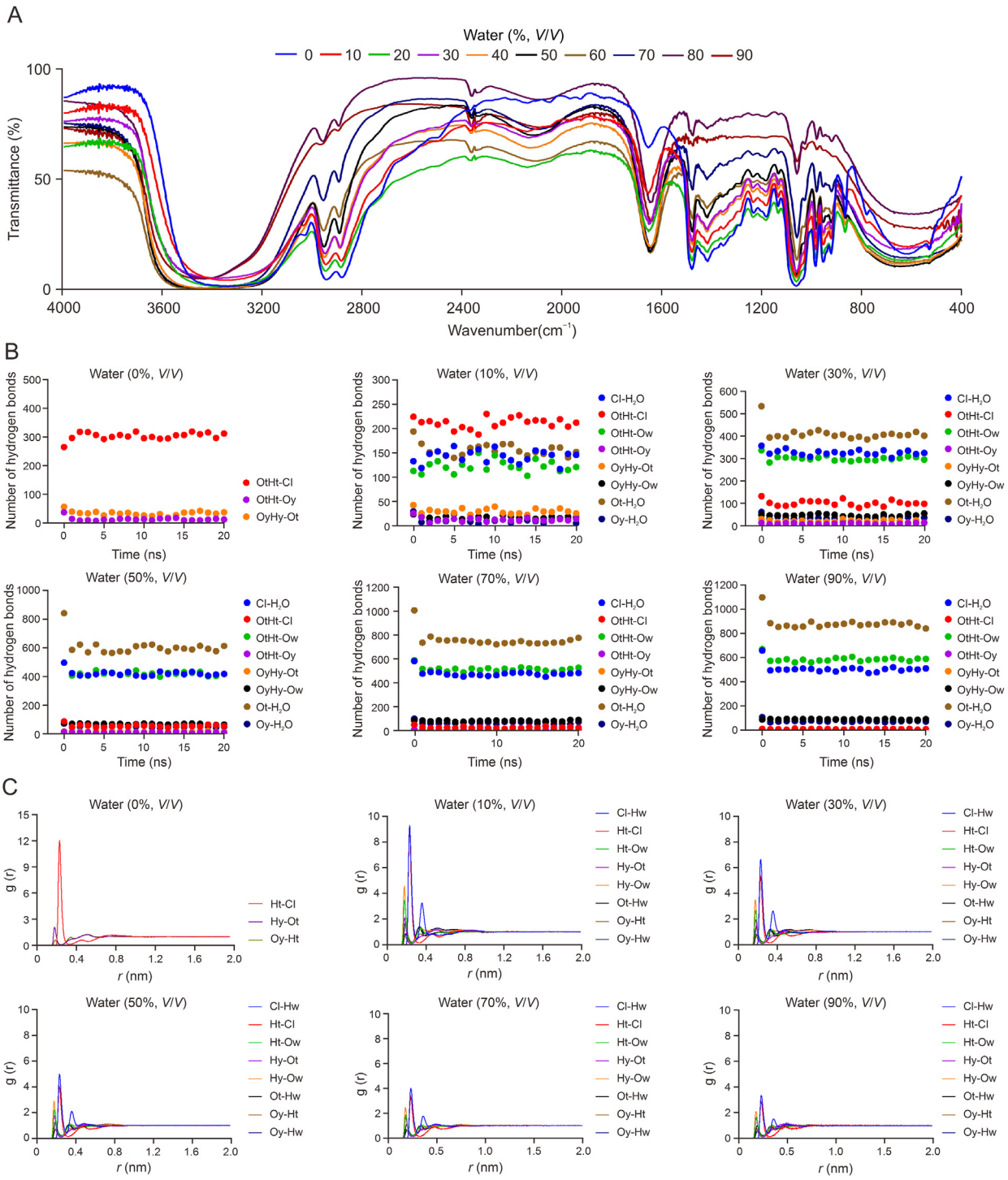

Fig. 2. Fourier transform Infrared (FTIR) and conventional molecular dynamics (CMD) simulations of DES-A10 (the optimum one) with different water conditions (A) comparison of FTIR of preferred DES-A10 under different water contents; (B) number of hydrogen bonds between hydrogen bond acceptor (HBA), hydrogen bond donor (HBD), and water with different water conditions; and (C) plots of the radial distribution function (RDF) of choline chloride, 1,3-propanediol, and water with different water conditions. The hydroxyl groups on choline are designated as Hy and Oy, the terminal oxygen and hydrogen atoms of 1,3-propanediol labeled are designated as Ot and Ht, and the hydrogen and oxygen atoms of water were designated as Hw and Ow, respectively.

and water, and between 1,3-propanediol and water, then constituted the framework of the entire hydrogen bond network. This also accounted for the observation that most of the solvent properties of the DESs diminished upon the addition of excessive water.

The radial distribution function (RDF), which indicates changes in particle density with respect to distance, was depicted in Fig. 2C for various conditions of water addition. The RDF exhibited three distinct peaks, which suggested the existence of a correlation between choline chloride and 1,3-propanediol within the DES system. The height of the significant pairs' peaks in the RDF indicated the formation of hydrogen bonds, aligning with prior conclusions. Concurrently, it was observed that the RDF values progressively

diminished with an increase in water content, signifying a weakening interaction between the components of the DES as the water molecule content rose. The findings collectively implied that the introduction of an appropriate quantity of water could enhance the hydrogen bond content within the DES system, which was advantageous for the extraction process. However, when the water content surpassed 50% (*V*/*V*), the addition of water was found to directly disrupt the DES structure, dissolve the HBA and HBD in water, and consequently decrease the extraction efficiency. Consequently, it was established that a DES, consisting of choline chloride and 1,3-propanediol at a molar ratio of 1:3.5, with water content of 30% (*V*/*V*), is optimal for the extraction of proanthocyanidins from Rhodiolae Crenulatae Radix et Rhizomes.

An assessment of different extraction conditions determined the most effective solid-to-liquid ratio to be 1:30, coupled with an extraction temperature of 40 °C and duration of 50 min. To refine this process, a Box-Behnken design and response surface methodology were employed, designing a three-factor, three-level experiment. This experiment varied the solid-to-liquid ratio, extraction temperature, and extraction time to gauge their impact on the yield of proanthocyanidins. The specific levels for each extraction factor and the detailed methodology can be found in Table S6. The primary goal was to optimize the content of proanthocyanidins in the extract using these tailored DES conditions.

The preparation process for proanthocyanidins from Rhodiolae Crenulatae Radix et Rhizomes extracted with DES was optimized. The Box-Behnken design-response surface methodology is used to conduct the experiments, as shown in Fig. S4 and Tables S7 and S8. The experimental results were analyzed using Design-Expert software. According to the response surface methodology, the results showed that the optimal extraction condition corresponded to the solid to liquid ratio of 1:30, extraction temperature of 40 °C, and extraction time of 50 min. The optimal extraction conditions were determined to achieve a maximum extraction rate of 29.80%, which significantly surpassed the extraction rate of 22.21% obtained with 70% acetone, demonstrating that DESs can serve as alternatives to organic reagents for more efficient proanthocyanidin extraction from Rhodiolae Crenulatae Radix et Rhizomes.

The results of UV and IR detections are shown in Fig. S5. UV and IR results suggested that the proanthocyanidins were mainly composed of catechin and epicatechin.

3.2. Construction of precursor ion scan list based on proanthocyanidin structural library

MDF was used to construct a scanning list of proanthocyanidin precursor ions, and the data-dependent acquisition (DDA) scanning mode was combined to realize the specific scanning of proanthocyanidins in the extract [38,39]. The proanthocyanidin oligomers are dominated by dimers, trimers, and tetramers, so that the composition of the possible oligomeric proanthocyanidins that may exist can be predicted from the structural units of flavan-3-ol based on different monomer numbers, different connection modes, and whether the galloyl groups are connected. Therefore, the structural composition of the type-B proanthocyanidin, which may exist, can be speculated according to the following formula:

$$a \times (C_{15}H_{14}O_5) + b \times (C_{15}H_{14}O_6) + c \times (C_{15}H_{14}O_7) + d \times (C_8H_8O_3) - 2 \times (n-1) + 2e$$

where $a/b/c = 0, 1, 2, 3, 4$, $d/e = 0, 1, 2$, and $n = 2, 3, 4$.

Possible dimers, trimers, and tetramers are summarized in Table S9. The results showed that 72 type-B OPCs may be present. Construction of the proanthocyanidin structural database included four main parts. First, a self-built database containing 75 proanthocyanidins was established based on a literature review. Second, the possible chemical composition of the 72 OPCs was calculated based on their proanthocyanidin structural units. In the third part, the proanthocyanidin components in Rhodiolae Crenulatae Radix et Rhizomes were detected via UHPLC-Orbitrap Exploris 120 MS, and the obtained data were processed via Compound Discovery to screen the mass number of mother nuclei with proanthocyanidin characteristics as the potential proanthocyanidin components (19). In the fourth part, the proanthocyanidins in Rhodiolae Crenulatae Radix et Rhizomes was also detected by UHPLC-Orbitrap Exploris 120 MS, and the obtained data were processed by Compound Discovery to screen the mass number of neutral loss (NL) with the structural feature of flavan-3-ols as the potential proanthocyanidins (43). The first and second sections describe the reported proanthocyanidins, whereas the third and fourth sections describe the underlying proanthocyanidins. After removing duplicate mass numbers from the four sections of the data, the remaining 162 mass numbers were organized into a table, which was used as the mass number of the theoretical precursor ions of the proanthocyanidins. After analyzing the data from UHPLC coupled with Orbitrap Exploris 120 MS for proanthocyanidins, we used SIEVE software to process the information, resulting in a table of 9,618 compound ions. To refine this list, we compared the detected proanthocyanidin ions with the integer mass numbers $[M-H]^-$ from a theoretical precursor ion table. From this comparison, we were able to exclude non-target compounds, reducing the list to 196 mass numbers. Further refinement was conducted by applying a dynamic mass defect filter (±10 mDa) to the remaining data, which aided in eliminating interference from non-target compounds. After deduplication of the data, we identified a final set of 156 mass numbers corresponding to proanthocyanidin precursor ions. This refined dataset is depicted in the distribution diagram in Fig. S6.

3.3. Characterization and identification of proanthocyanidins in Rhodiolae Crenulatae Radix et Rhizomes

The HCD-MS^2 data collected in the negative ion mode were compared and analyzed with the reference substance, constructed proanthocyanidin structural library, and combined literature to systematically characterize the proanthocyanidin component in Rhodiolae Crenulatae Radix et Rhizomes. Finally, 50 components were identified (or deduced), including seven monomers (four of which were compared with the standard substance), 22 dimers (two of which were compared with the standard substance), 20 trimers (one of which was compared with the standard substance), and 1 tetramer.

Proanthocyanidin monomers mainly exhibit 1,4-bond cleavage in the C ring of the flavan-3-ols structural unit and 1,2-bond and 1,3-bond cleavage in the A ring. In addition to the common fragmentation forms of monomers, proanthocyanidin polymers exhibit heterocyclic ring fission (HRF) and retro-Diels-Alder (RDA) reaction of flavan-3-ol, and quinone methide (QM) cleavage of the interflavan bond [31,42]. When the proanthocyanidin polymer was subjected to QM cleavage, the E-unit $[M_E-5H]^-$ fragments of type A proanthocyanidins were usually the characteristic fragment of *m*/*z* 285 (epicatechin/catechin (EC)), *m*/*z* 301 (epigallocatechin/gallocatechin (EG)), and *m*/*z* 269 (epiafzelechin/afzelechin (EA)). The common T-unit $[M_T-H]^-$ fragments of procyanidin type B were *m*/*z* 289 (EC), *m*/*z* 305 (EG), and *m*/*z* 273 (EA), and the E-unit $[M_E-3H]^-$ fragments were *m*/*z* 287 (EC), *m*/*z* 303 (EG), and *m*/*z* 271 (EA) [31,43–45]. To facilitate the presentation of the identification (or derivation) results, catechin or epicatechin is represented by EC, gallic acid catechin (epigallocatechin) or epigallocatechin (epigallocatechin) is represented by EG, and avermectin or epi-

avermectin is represented by EA. The identification results are presented in Table S10. Identification (or derivation) of each proanthocyanidin type is discussed below.

3.3.1. Monomer

Compound 3 (retention time (t_R) = 7.60 min, $C_{15}H_{13}O_6$) is shown in Fig. 3A with the *m/z* 289 ($[M-H]^-$) yielding a fragment of *m/z* 245 ($[M-H-CO_2]^-$) after the loss of CO_2 (NL: 44 Da). When *m/z* 289 ($[M-H]^-$) lost two C_2H_2O (NL: 44 Da), $C_6H_6O_2$ (NL: 110 Da), and $C_8H_8O_3$ (NL: 152 Da), fragments of *m/z* 205 ($[M-H-2C_2H_2O]^-$), *m/z* 179 ($[M-H-C_6H_6O_2]^-$), and *m/z* 137 ($[M-H-C_8H_8O_3]^-$) were obtained. According to the different fragmentation of the fragments, it could be determined that **compound 3** had multiple cleavage forms. After comparison with the secondary fragments and t_R of the reference substance, **compound 3** was identified as epicatechin.

Compound 4 (t_R = 13.71 min, $C_{22}H_{17}O_{10}$) is shown in Fig. 3B. When *m/z* 441 ($[M-H]^-$) underwent a loss of $C_8H_8O_3$ (NL: 152 Da), the characteristic fragment of *m/z* 289 ($[M-H-C_8H_8O_3]^-$) was obtained, and the fragment of *m/z* 245 ($[M-H-C_8H_8O_3-CO_2]^-$) was obtained after the continuous loss of one CO_2 molecule (NL: 44 Da). Simultaneously, the fragment of *m/z* 169 in MS^2 indicated the possibility of a gallic acid radical in the structure. When a gallic acid group (NL: 170 Da) was lost in peak *m/z* 441 ($[M-H]^-$), a fragment *m/z* 271 ($[M-H-C_7H_6O_5]^-$) was obtained. When the C-1 and C-4 were broken in the C ring, the flavonoid characteristic fragment *m/z* 125 ($^{1,4}A^-$) was obtained. After thorough comparison of the secondary fragment patterns and t_Rs with those of a standard reference, **Compound 4** was conclusively identified as epicatechin-3-gallate (ECG).

3.3.2. Dimer

The proanthocyanidin dimers in Rhodiolae Crenulatae Radix et Rhizomes mainly include type-B procyanidin (EC-EC), procaine (EG-EG), a large amount of proanthocyanidins with gallic acid, and a small amount of type-A procyanidins (EC-A-EC) and proanthocyanidins (EC-A-EG). A representative dimer was selected to describe the derivation and identification processes.

The MS^2 of **compound 17** (t_R = 11.91 min, $C_{30}H_{23}O_{12}$) is shown in Fig. 3C, which mainly shows three forms of fragmentation. 1) HRF fragmentation of $[M-H]^-$ *m/z* 575 occurs to lose $C_6H_6O_3$ (NL: 126 Da), producing the fragment of *m/z* 449 ($[M-H-C_6H_6O_3]^-$). 2) RDA fragmentation of $[M-H]^-$ occurred: $C_8H_8O_3$ (NL: 152 Da) was lost, and the fragment of *m/z* 423 ($[M-H-C_8H_8O_3]^-$) was generated. 3) QM cleavage occurred in $[M-H]^-$, and after lost its T-unit, only *m/z* 285 ($[M_E-5H]^-$) E-unit was left, suggesting that the compound was type-A proanthocyanidin subjected to HRF and RDA cleavage. **Compound 17** was identified as proanthocyanidin A1 (OPC-A1) after comparison with secondary fragments and t_Rs of the standard reference.

Similarly, MS^2 of **compound 9** (t_R = 6.62 min, $C_{30}H_{25}O_{12}$) is shown in Fig. 3D, and two main forms of fragmentation are observed. 1) RDA fragmentation of *m/z* 577 ($[M-H]^-$) lead to a loss $C_8H_8O_3$ (NL: 152 Da) and producing the fragment of *m/z* 425 ($[M-H-C_8H_8O_3]^-$). This was followed by the loss of H_2O, yielding a fragment of *m/z* 407 ($[M-H-C_8H_8O_3-H_2O]^-$). 2) $[M-H]^-$ underwent QM cleavage, leaving only *m/z* 289 ($[M_T-H]^-$) T-unit, suggesting that the compound was type-B proanthocyanidin subjected to RDA cleavage. **Compound 9** was identified as procyanidin B2 (OPC-B2) by comparing the t_Rs of the secondary fragments against the standard.

Similarly, the MS^2 of **compound 12** (t_R = 7.94 min, $C_{37}H_{29}O_{16}$) is shown in Fig. 3E. Three main forms of fragmentation were observed. 1) RDA fragmentation of *m/z* 729 ($[M-H]^-$) occurred and $C_8H_8O_3$ (NL: 152 Da) was lost, producing the fragment of *m/z* 577 ($[M-H-C_8H_8O_3]^-$) continues to fragment under sustained high energy collisions. This not only produces a fragment of *m/z* 559 ($[M-H-C_8H_8O_3-H_2O]^-$) but also continues to RDA cleavage and lose $C_8H_8O_3$ (NL: 152 Da). The generation of *m/z* 425 ($[M-H-2C_8H_8O_3]^-$), which continues to fragment losing H_2O, generates a fragment of *m/z* 407 ($[M-H-2C_8H_8O_3-H_2O]^-$). 2) QM cleavage occurred in $[M-H]^-$, and after the compound lost its E-unit, only *m/z* 289 ($[M_T-H]^-$) T-unit was left, suggesting that the compound was type-B proanthocyanidin subjected to RDA cleavage. The fragment *m/z* 169 suggested the existence of a gallic acid radical in the structure. Based on the characteristic fragments and cleavage pattern, **compound 12** was identified as a type-B procyanidin with gallic acid ((EC-EC)-g).

3.3.3. Trimer

Similar to dimers, proanthocyanidin trimers in Rhodiolae Crenulatae Radix et Rhizomes mainly include type-B procyanidin (EC-EC-EC), procaine (EG-EG-EG), large amounts of proanthocyanidins with gallic acid, and small amounts of type-A procyanidin (EC-A-EC). A representative trimer was selected to describe the derivation identification process.

Fig. 3F is MS^2 of **compound 33** (t_R = 8.69 min, $C_{45}H_{37}O_{18}$). The fragment ion information indicates that this compound undergoes two types of fragmentation. 1) QM cleavage occurs directly at *m/z* 865 ($[M-H]^-$), and loses T-unit to generate the characteristic fragment of *m/z* 289 ($[M_T-H]^-$). After continuing the QM cleavage, only E-unit remains to produce *m/z* 287 ($[M_E-3H]^-$), indicating that this compound is a single-chain type-B procyanidin, and there are more than two flavan-3-ols structural units at the same time. 2) $[M-H]^-$ loses $C_{15}H_{12}O_6$ after QM cleavage, producing the fragment of *m/z* 577 ($[M-H-C_{15}H_{12}O_6]^-$) and continues high-energy collision. RDA fragmentation leads to loss $C_8H_8O_3$ (NL: 152 Da). The fragment of *m/z* 425 ($[M-H-C_{15}H_{12}O_6-C_8H_8O_3]^-$) is generated and fragmentation continues with the loss of H_2O, yielding the fragment of *m/z* 407 ($[M-H-C_{15}H_{12}O_6-C_8H_8O_3-H_2O]^-$). **Compound 33** was identified as procyanidin C1 (OPC-C1) based on fragment information and possible fragmentation patterns, as well as secondary fragments and t_R of the standard.

Fig. 3G is the same as Fig. 3F, but we can find fragments *m/z* 169, suggesting the existence of a gallic acid radical in the structure. Based on the characteristic fragments and cleavage pattern, **compound 37** was identified as a type-B procyanidin with gallic acid ((EC-EC-EC)-g).

3.3.4. Tetramer

The tetrameric proanthocyanidins in Rhodiolae Crenulatae Radix et Rhizomes are type-B procyanidin. The derivation and identification processes are as follows: Fig. 3H shows the two-stage mass spectrum of **compound 50** (t_R = 9.67 min, $C_{60}H_{49}O_{24}$). The fragment ion information in the figure indicates that the compound underwent three main types of fragmentation. 1) QM cleavage occurs directly at *m/z* 1,153 ($[M-H]^-$), and the compound loses T-unit to generate the characteristic fragment of *m/z* 289 ($[M_T-H]^-$). QM cleavage continues until only the remaining E-unit produces the characteristic fragment of *m/z* 287 ($[M_E-3H]^-$), suggesting that the compound is a single-chain procyanidin type-B and there is more than two flavan-3-ols structural units at the same time. 2) $[M-H]^-$ loses $C_{15}H_{12}O_6$ after QM cleavage directly, and HRF fragmentation continue to producing the fragment of *m/z* 739 ($[M-H-C_{15}H_{12}O_6-C_6H_6O_3]^-$). 3) $[M-H]^-$ underwent continuous QM cleavage directly, losing two $C_{15}H_{12}O_6$, producing the fragment of *m/z* 577 ($[M-H-2C_{15}H_{12}O_6]^-$), and RDA fragmentation continued with the loss of H_2O, producing the fragment of *m/z* 407

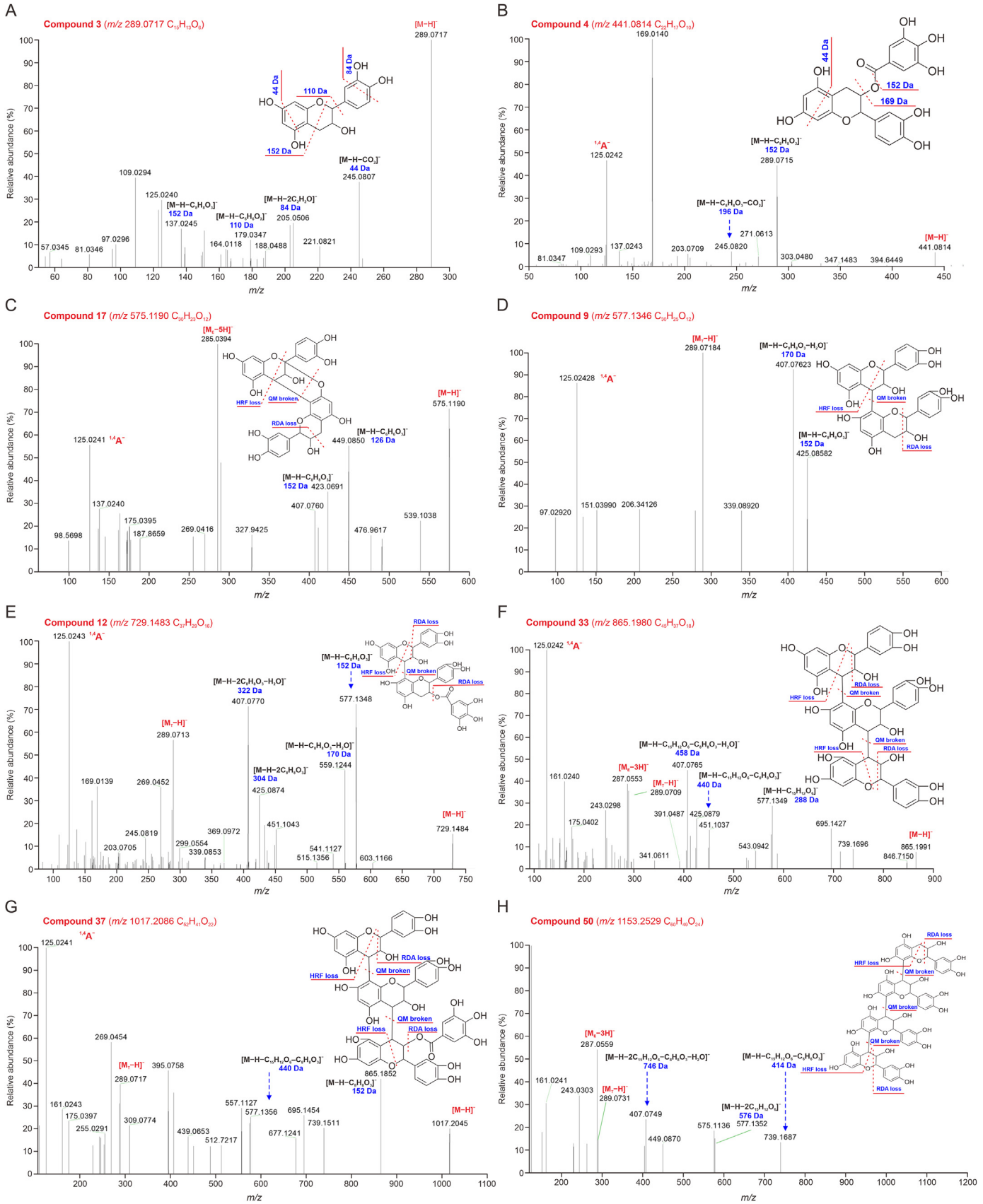

Fig. 3. Fragmentation pathway analysis of proanthocyanidins: (A–B) Fragmentation pathway analysis of monomer: **compounds 3** (A) and **4** (B); (C–E) fragmentation pathway analysis of dimer: **compounds 17** (C), **9** (D), and **12** (E); (F, G) fragmentation pathway analysis of trimer: **compounds 33** (F) and **37** (G); and (H) fragmentation pathway analysis of tetramer: **compound 50**. HRF: heterocyclic ring fission; QM: quinone methide; RDA: retro-Diels-Alder.

($[M-H-2C_{15}H_{12}O_6-C_8H_8O_3-H_2O]^-$). Based on the fragment information and fragmentation pattern, **compound 50** was identified as a type-B procyanidin (EC-EC-EC-EC).

Based on the identification results, we found that the proanthocyanidins extracted with DES consisted of seven monomers (14%), 22 dimers (44%), 20 trimers (40%), and a tetramer (2%), most of which were mainly composed of procyanidin (61%) linked to gallic acid, a small amount of procyanidin (23%), procaine (14%), and other types of proanthocyanidins (2%). As shown in Fig. 4, the dimers were mainly composed of six types of proanthocyanidins: six (EC-EC)-2g, five (EC-EC)-g, two (EC-EG)-g, four EC-A-EC, four EC-EC, and one EC-A-EG. The trimers mainly consisted of five types of proanthocyanidins: eight (EC-EC-EC)-2g, six (EC-EC-EC)-g, one EC-A-EC-EC, three EC-EC-EC, and two EG-EG-EG, respectively. Only one EC-EC tetramer was identified. Most were type B proanthocyanidins (88%), and a few type A proanthocyanidins (12%) were also present. The aforementioned results indicated that proanthocyanidins, mainly composed of oligomers in Rhodiolae Crenulatae Radix et Rhizomes, were mainly composed of procyanidin.

Simultaneously, under high-energy collisions, the proanthocyanidin in Rhodiolae Crenulatae Radix et Rhizomes generally undergoes QM cleavage, i.e., it is fractured into a proanthocyanidin monomer structure. When QM cleavage occurs, the characteristic fragments of $[M_T-H]^-$ (EC = 289, EG = 305, and EA = 273) and $[M_E-3H]^-$ (EC = 287, EG = 303, and EA = 271) were often present in the secondary fragment of type B proanthocyanidin, and the characteristic fragment of $[M_E-5H]^-$ (EC = 285, EG = 301, and EA = 269) was present in the secondary fragment of type A proanthocyanidin. The simultaneous presence of the T-unit or E-unit in the secondary fragment suggests that the compound may be a trimer with a higher degree of polymerization. In addition to QM cleavage, proanthocyanidins are also susceptible to RDA and HRF fragmentation. When the NL was 152 Da, EC underwent RDA

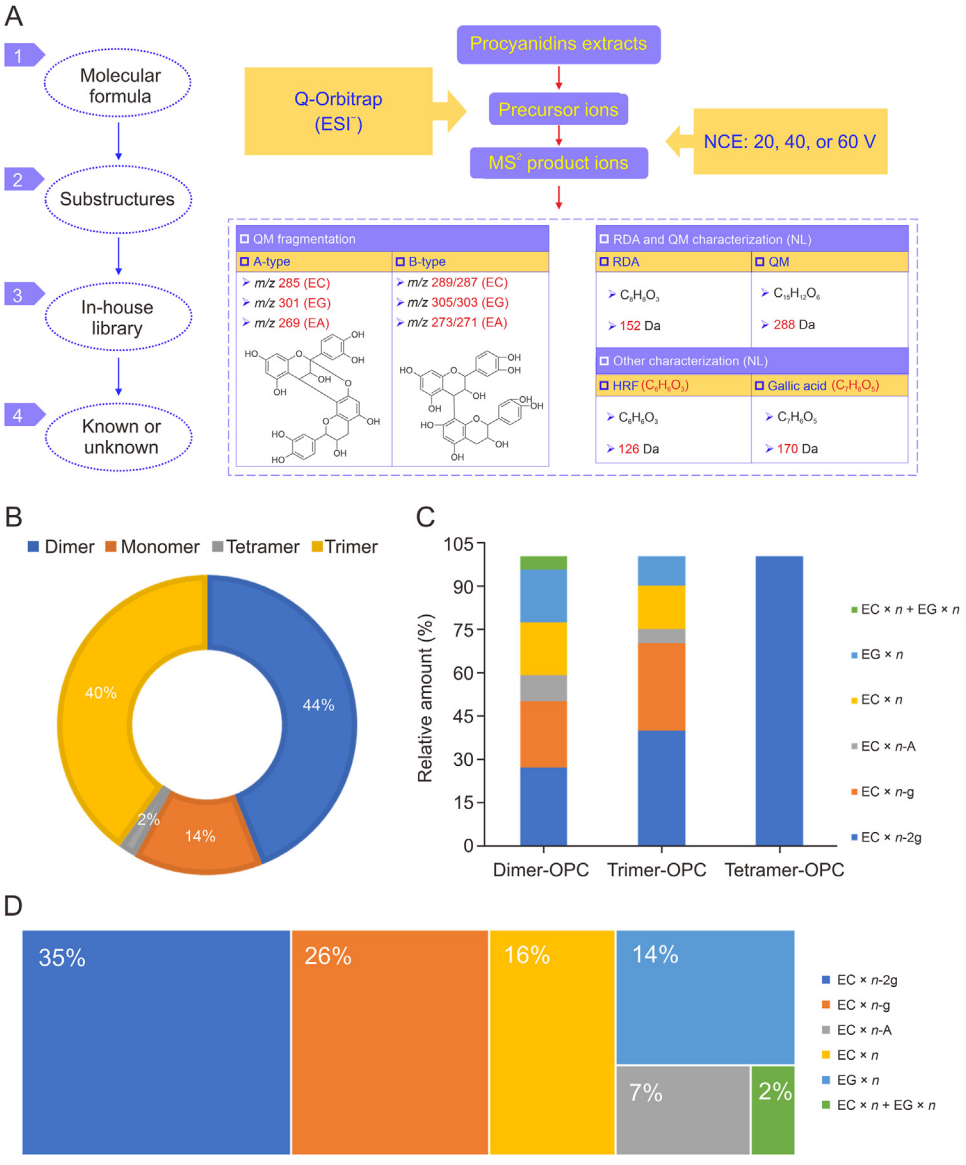

Fig. 4. The content distribution of oligomeric proanthocyanidins (OPCs). (A) A general flowchart for the rapid characterization of proanthocyanidins based on the diagnostic fragmentation information, according to the negative high energy collision dissociation (HCD)-mass spectrometry $(MS)^2$ data. (B) The proportion of proanthocyanidins with different degrees of polymerization. (C) The specific type of proanthocyanidin in each oligomer. (D) The proportion of various types of proanthocyanidins. ESI: electrospray ionization; NCE: normalized collision energy; QM: quinone methide; EC: epicatechin/catechin; EG: epigallocatechin/gallocatechin; EA: epiafzelechin/afzelechin; RDA: retro-Diels-Alder; NL: neutral loss; HRF: heterocyclic ring fission.

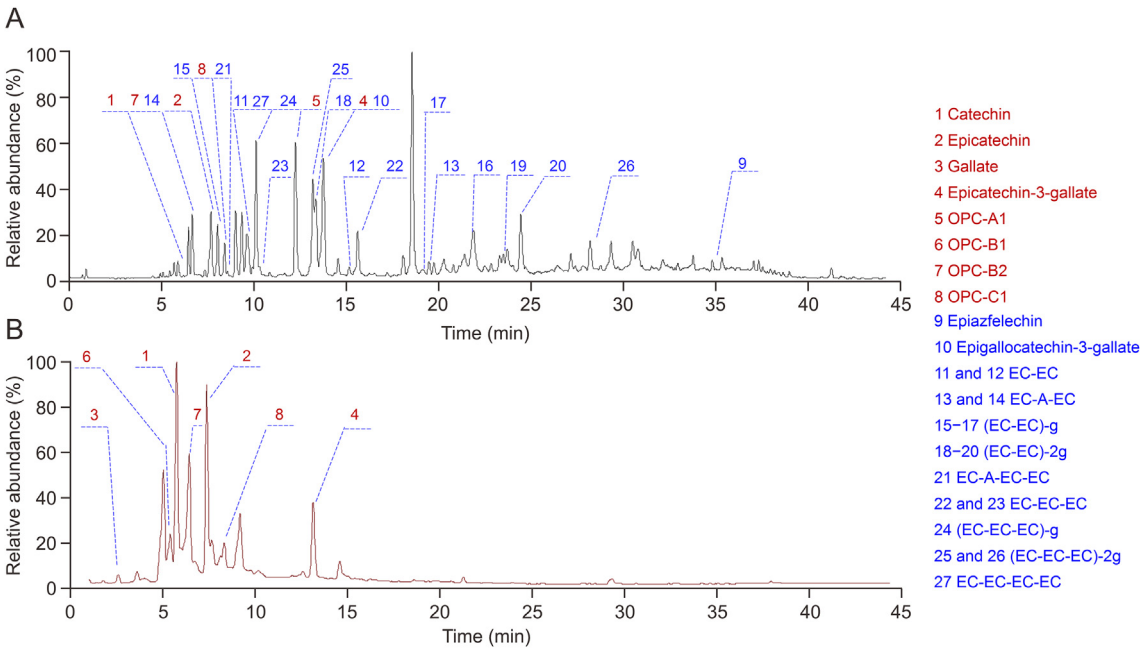

Fig. 5. The comparison of proanthocyanidins from Rhodiolae Crenulatae Radix et Rhizomes with United States Pharmacopeia (USP) oligomeric proanthocyanidins (OPCs) standard extracted from grape seeds: (A) the total ion chromatogram of the proanthocyanidins from Rhodiolae Crenulatae Radix et Rhizomes and (B) the total ion chromatogram of USP OPCs standard extracted from grape seeds. EC: epicatechin/catechin; EC-A-EC: epicatechin/catechin-A-type-epicatechin/catechin.

cleavage. When the NL was 168 Da, RDA cleavage occurred in the EG. When a NL of 136 Da occurred, the EA underwent RDA cleavage. RDA fragmentation is typically accompanied by the loss of H_2O. Simultaneously, the NL of 126 Da suggests that EC, EG, and EA units undergo HRF. The detection of a fragment with *m*/*z* 169 among the secondary fragments points to the presence of gallic acid moieties within the structure.

The OPCs extracted from Rhodiolae Crenulatae Radix et Rhizomes using DES were compared with the United States Pharmacopeia (USP) standard of OPCs derived from grape seeds, under identical analytical conditions. As depicted in Fig. 5, the variety of OPCs present in Rhodiolae Crenulatae Radix et Rhizomes (Fig. 5A) is significantly more diverse than that found in grape seeds (Fig. 5B). In addition to containing the same proanthocyanidin types, such as procyanidins and prodelphinidins, specified by the USP, Rhodiolae Crenulatae Radix et Rhizomes also boasts an abundance of OPCs conjugated with gallic acid groups. Moreover, these polymers possess a higher number of hydroxyl groups, suggesting that the OPCs from Rhodiolae Crenulatae Radix et Rhizomes may exhibit more potent antioxidant activities than those extracted from grape seeds.

4. Conclusion

An optimal extraction system for proanthocyanidins from Rhodiolae Crenulatae Radix et Rhizomes was established using a DES composed of choline chloride and 1,3-propanediol at a molar ratio of 1:3.5 and water content of 30% (*V*/*V*). This system was identified through a combination of single-factor experimentation and response surface methodology. For the analysis, a UHPLC/Orbitrap Exploris 120 HRMS was employed to create an ion scan list for proanthocyanidin precursors. This list was derived from a structural library and utilized the MDF algorithm. The scan mode Full MS/dd-MS^2 was implemented, activating the "if idle pick others" and DE features for efficiency. Targeted and non-targeted characterization of Rhodiolae Crenulatae Radix et Rhizomes's proanthocyanidins was achieved, identifying 50 components within the extracts. These ranged from monomers to tetramers, indicating a complex OPC profile. The extraction efficacy of the DES was found to be comparable to that of acetone and superior to conventional solvents such as methanol and ethanol. This suggests that the DES can serve as an environmentally friendly and effective substitute for acetone in extraction processes. Additionally, the comprehensive ion scanning strategy enabled simultaneous detection of known proanthocyanidin components and potential new chemical entities. This approach has allowed for a thorough characterization of Rhodiolae Crenulatae Radix et Rhizomes proanthocyanidins and has provided valuable reference data for further analytical and identification work, as well as for exploring the phytochemistry of other plant species.

CRediT author statement

Li Jia: Methodology, Investigation, Data curation, Writing - Original draft preparation; **Liming Wang:** Data curation, Writing - Reviewing and Editing, Visualization; **Xiaoxiao Zhang:** Data curation, Formal analysis; **Qingrui Zhang:** Data curation, Formal analysis, Investigation; **Peng Lei:** Data curation, Visualization; **Yanxu Chang:** Writing - Reviewing and Editing, Supervision; **Lifeng Han**, **Xin Chai**, **Wenzhi Yang**, and **Yuefei Wang:** Writing - Reviewing and Editing, Supervision; **Miaomiao Jiang:** Resources, Writing - Reviewing and Editing, Conceptualization, Supervision, Funding acquisition.

Declaration of competing interest

The authors declare that there are no conflicts of interest.

Acknowledgments

This work was supported by the Science and Technology Program of Tianjin in China (Grant No.: 23ZYJDSS00030) and the Science and Technology Project of Haihe Laboratory of Modern

Chinese Medicine, China (Grant Nos.: 22HHZYSS00007 and 22HHZYJC00003).

Appendix A. Supplementary data

Supplementary data to this article can be found online at https://doi.org/10.1016/j.jpha.2024.101002.

References

[1] D. Ma, L. Wang, Y. Jin, et al., Chemical characteristics of *Rhodiola crenulata* and its mechanism in acute mountain sickness using UHPLC-Q-TOF-MS/MS combined with network pharmacology analysis, J. Ethnopharmacol. 294 (2022), 115345.

[2] X. Bai, X. Deng, G. Wu, et al., *Rhodiola* and salidroside in the treatment of metabolic disorders, Mini Rev. Med. Chem. 19 (2019) 1611–1626.

[3] W. Pu, M. Zhang, R. Bai, et al., Anti-inflammatory effects of *Rhodiola rosea* L.: A review, Biomed. Pharmacother. 121 (2020), 109552.

[4] H.I. Chen, H.C. Ou, C.Y. Chen, et al., Neuroprotective effect of *Rhodiola crenulata* in D-galactose-induced aging model, Am. J. Chin. Med. 48 (2020) 373–390.

[5] D.N. Olennikov, N.K. Chirikova, A.G. Vasilieva, et al., LC-MS profile, gastrointestinal and gut microbiota stability and antioxidant activity of *Rhodiola rosea* herb metabolites: A comparative study with subterranean organs, Antioxidants 9 (2020), 526.

[6] S. Toro-Uribe, M. Herrero, E.A. Decker, et al., Preparative separation of procyanidins from cocoa polyphenolic extract: Comparative study of different fractionation techniques, Molecules 25 (2020), 2842.

[7] J.F. Hammerstone, S.A. Lazarus, A.E. Mitchell, et al., Identification of procyanidins in cocoa (*Theobroma* cacao) and chocolate using high-performance liquid chromatography/mass spectrometry, J. Agric. Food Chem. 47 (1999) 490–496.

[8] N. Hellenbrand, J. Sendker, M. Lechtenberg, et al., Isolation and quantification of oligomeric and polymeric procyanidins in leaves and flowers of Hawthorn (*Crataegus* spp.), Fitoterapia 104 (2015) 14–22.

[9] T. Song, P. Wang, C. Li, et al., Salidroside simultaneously reduces *de novo* lipogenesis and cholesterol biosynthesis to attenuate atherosclerosis in mice, Biomed. Pharmacother. 134 (2021), 111137.

[10] H. Chen, J. Zhu, Y. Le, et al., Salidroside inhibits doxorubicin-induced cardiomyopathy by modulating a ferroptosis-dependent pathway, Phytomedicine 99 (2022), 153964.

[11] L. Rong, Z. Li, X. Leng, et al., Salidroside induces apoptosis and protective autophagy in human gastric cancer AGS cells through the PI3K/Akt/mTOR pathway, Biomed. Pharmacother. 122 (2020), 109726.

[12] S. Zhao, L. Zhang, C. Yang, et al., Procyanidins and Alzheimer's disease, Mol. Neurobiol. 56 (2019) 5556–5567.

[13] E.A. Rue, M.D. Rush, R.B. van Breemen, Procyanidins: A comprehensive review encompassing structure elucidation via mass spectrometry, Phytochem. Rev. 17 (2018) 1–16.

[14] Z. Chen, J. Tan, J. Qin, et al., Effects of lotus seedpod oligomeric procyanidins on the inhibition of AGEs formation and sensory quality of tough biscuits, Front. Nutr. 9 (2022), 1031550.

[15] Y. Sui, J. Shi, S. Cai, et al., Metabolites of procyanidins from *Litchi chinensis* pericarp with xanthine oxidase inhibitory effect and antioxidant activity, Front. Nutr. 8 (2021), 676346.

[16] D. Ferreira, D. Slade, Oligomeric proanthocyanidins: Naturally occurring *O*-heterocycles, Nat. Prod. Rep. 19 (2002) 517–541.

[17] A. Tuominen, M. Karonen, Variability between organs of proanthocyanidins in *Geranium sylvaticum* analyzed by off-line 2-dimensional HPLC-MS, Phytochemistry 150 (2018) 106–117.

[18] J.A. Kennedy, G.P. Jones, Analysis of proanthocyanidin cleavage products following acid-catalysis in the presence of excess phloroglucinol, J. Agric. Food Chem. 49 (2001) 1740–1746.

[19] T. Mohana, A.V. Navin, S. Jamuna, et al., Inhibition of differentiation of monocyte to macrophages in atherosclerosis by oligomeric proanthocyanidins – *In-vivo* and *in-vitro* study, Food Chem. Toxicol. 82 (2015) 96–105.

[20] N. Hellenbrand, M. Lechtenberg, F. Petereit, et al., Isolation and quantification of oligomeric and polymeric procyanidins in the aerial parts of St. John's wort (*Hypericum perforatum*), Planta Med. 81 (2015) 1175–1181.

[21] K. Schötz, M. Nöldner, Mass spectroscopic characterisation of oligomeric proanthocyanidins derived from an extract of *Pelargonium sidoides* roots (EPs 7630) and pharmacological screening in CNS models, Phytomedicine 14 (2007) 32–39.

[22] W. Tao, H. Pan, H. Jiang, et al., Extraction and identification of proanthocyanidins from the leaves of persimmon and loquat, Food Chem. 372 (2022), 130780.

[23] J. Cao, L. Chen, M. Li, et al., Efficient extraction of proanthocyanidin from *Ginkgo biloba* leaves employing rationally designed deep eutectic solvent-water mixture and evaluation of the antioxidant activity, J. Pharm. Biomed. Anal. 158 (2018) 317–326.

[24] A.R. Jesus, L. Meneses, A.R.C. Duarte, et al., Natural deep eutectic systems, an emerging class of cryoprotectant agents, Cryobiology 101 (2021) 95–104.

[25] A.P. Abbott, K.J. Edler, A.J. Page, Deep eutectic solvents-The vital link between ionic liquids and ionic solutions, J. Chem. Phys. 155 (2021), 150401.

[26] J.M. Hartley, S. Scott, Z. Dilruba, et al., Iodine speciation in deep eutectic solvents, Phys. Chem. Chem. Phys. 24 (2022) 24105–24115.

[27] M. Zhang, X. Zhang, Y. Liu, et al., Insights into the relationships between physicochemical properties, solvent performance, and applications of deep eutectic solvents, Environ. Sci. Pollut. Res. Int. 28 (2021) 35537–35563.

[28] J.K.U. Ling, K. Hadinoto, Deep eutectic solvent as green solvent in extraction of biological macromolecules: A review, Int. J. Mol. Sci. 23 (2022), 3381.

[29] L.E. Meyer, M.B. Andersen, S. Kara, A deep eutectic solvent thermomorphic Multiphasic system for biocatalytic applications, Angew. Chem. Int. Ed. Engl. 61 (2022), e202203823.

[30] F. Wang, J. Zhang, P. Yin, et al., Rapid identification of polyphenols in Kudiezi injection with a practical technique of mass defect filter based on high-performance liquid chromatography coupled with linear ion trap/orbitrap mass spectrometry, Anal. Methods 6 (2014) 3515–3523.

[31] L.-Z. Lin, J. Sun, P. Chen, et al., UHPLC-PDA-ESI/HRMSn profiling method to identify and quantify oligomeric proanthocyanidins in plant products, J. Agric. Food Chem. 62 (2014) 9387–9400.

[32] Y. Dai, E. Rozema, R. Verpoorte, et al., Application of natural deep eutectic solvents to the extraction of anthocyanins from *Catharanthus roseus* with high extractability and stability replacing conventional organic solvents, J. Chromatogr. A 1434 (2016) 50–56.

[33] Y. Dai, G.J. Witkamp, R. Verpoorte, et al., Natural deep eutectic solvents as a new extraction media for phenolic metabolites in *Carthamus tinctorius* L, Anal. Chem. 85 (2013) 6272–6278.

[34] Z. Yang, Natural deep eutectic solvents and their applications in biotechnology, Adv, Biochem. Eng. 168 (2019) 31–59.

[35] M. Ruesgas-Ramón, M.C. Figueroa-Espinoza, E. Durand, Application of deep eutectic solvents (DES) for phenolic compounds extraction: Overview, challenges, and opportunities, J. Agric. Food Chem. 65 (2017) 3591–3601.

[36] M.H. Zainal-Abidin, M. Hayyan, A. Hayyan, et al., New horizons in the extraction of bioactive compounds using deep eutectic solvents: A review, Anal. Chim. Acta 979 (2017) 1–23.

[37] N. Guo, P. Kou, Y. Jiang, et al., Natural deep eutectic solvents couple with integrative extraction technique as an effective approach for mulberry anthocyanin extraction, Food Chem. 296 (2019) 78–85.

[38] N. Symma, A. Hensel, Advanced analysis of oligomeric proanthocyanidins: Latest approaches in liquid chromatography and mass spectrometry based analysis, Phytochem. Rev. 21 (2022) 809–833.

[39] L. Jia, H. Wang, X. Xu, et al., An off-line three-dimensional liquid chromatography/Q-Orbitrap mass spectrometry approach enabling the discovery of 1561 potentially unknown ginsenosides from the flower buds of *Panax ginseng*, Panax *quinquefolius* and *Panax notoginseng*, J. Chromatogr. A 1675 (2022), 463177.

[40] S. Rozas, C. Benito, R. Alcalde, et al., Insights on the water effect on deep eutectic solvents properties and structuring: The archetypical case of choline chloride + ethylene glycol, J. Mol. Liq. 344 (2021), 117717.

[41] A. Shishov, S. Gagarionova, A. Bulatov, Deep eutectic mixture membrane-based microextraction: HPLC-FLD determination of phenols in smoked food samples, Food Chem. 314 (2020), 126097.

[42] A.P. Neilson, S.F. O'Keefe, B.W. Bolling, High-molecular-weight proanthocyanidins in foods: Overcoming analytical challenges in pursuit of novel dietary bioactive components, Annu. Rev. Food Sci. Technol. 7 (2016) 43–64.

[43] A. Rauf, M. Imran, T. Abu-Izneid, et al., Proanthocyanidins: A comprehensive review, Biomed. Pharmacother. 116 (2019), 108999.

[44] Y. Takahata, M. Ohnishi-Kameyama, S. Furuta, et al., Highly polymerized procyanidins in brown soybean seed coat with a high radical-scavenging activity, J. Agric. Food Chem. 49 (2001) 5843–5847.

[45] M. Bensa, V. Glavnik, I. Vovk, Flavan-3-ols and proanthocyanidins in Japanese, Bohemian and giant knotweed, Plants 10 (2021), 402.